Articles

Fabrication and Characterization of Multilayer Ultrathin Films of Exfoliated MnO_2 Nanosheets and Polycations

Lianzhou Wang,[†] Yoshitomo Omomo,[†] Nobuyuki Sakai,[†] Katsutoshi Fukuda,[†,‡] Izumi Nakai,[‡] Yasuo Ebina,[†,§] Kazunori Takada,[†,§] Mamoru Watanabe,[†] and Takayoshi Sasaki*[,†,§]

Advanced Materials Laboratory, National Institute for Materials Science, 1-1 Namiki, Tsukuba, Ibaraki 305-0044, Japan, Department of Applied Chemistry, Tokyo University of Science, 1-3 Kagurazaka, Shinjuku, Tokyo, 162-8601, Japan, and CREST, Japan Science and Technology Corporation (JST)

Received March 24, 2003. Revised Manuscript Received May 15, 2003

Multilayer ultrathin films composed of exfoliated nanosheets of manganese oxide and poly(diallyldimethylammonium) (PDDA) ions have been fabricated onto various substrates via electrostatic self-assembly technique. Dense monolayer coverage of the substrate surface by the nanosheets was confirmed by atomic force microscopy. UV−vis absorption spectroscopy provided evidence for subsequent growth of multilayer film, exhibiting progressive enhancement of optical absorption due to manganese oxide nanosheets. Evolution of a Bragg peak in the layer-by-layer deposition process also supported the growth of a nanostructured film of PDDA/MnO_2 nanosheets with a repeating periodicity of ca. 0.9 nm. Fourier transform infrared spectroscopy and X-ray photoelectron spectroscopy revealed the inorganic−organic hybrid nature of the obtained multilayer assemblies. Calcination of the films at temperatures above 500 °C removed the polycations, yielding an ultrathin film of manganese oxide Mn_2O_3. Cyclic voltammogram measurements revealed one reduction peak and two oxidation peaks for a monolayer film, which are attributable to the electrochemical conversion between Mn^{III} and Mn^{IV} in manganese oxide nanosheets.

Introduction

Manganese oxides have attracted considerable attention because of their wide range of electric, magnetic, catalytic, ion-exchange, and photocatalytic properties.[1−6] Manganese oxides in various forms and crystal structures, such as clusters, nanowires, spinel, layered, and perovskite structures, have been intensively investigated in terms of their synthesis and for the exploration of their physicochemical properties.[4,6,7−10] On the other hand, there has been increasing interest in thin films of manganese oxides because they are suitable for optical, electrochemical, and electronic studies, as well as their applications.[11−13] Fabrication of MnO_2 thin films has involved brushing−heating, sol−gel, and spin/dip coating procedures,[14−16] which generally yield thin films

* Corresponding author. Fax: +81-29-854-9061. E-mail: sasaki.takayoshi@nims.go.jp.
[†] National Institute for Materials Science.
[‡] Tokyo University of Science.
[§] CREST, Japan Science and Technology Corporation (JST).

(1) Shen Y.-F.; Zerger, R. P.; DeGuzman, R. N.; Suib, S. L.; McCurdy, L.; Potter, D. I.; O'Young, C. L. *Science* **1993**, *260*, 511.
(2) Yan, Y.-G.; Bein, T. *Chem. Mater.* **1993**, *5*, 905.
(3) Feng, Q.; Kanoh, H.; Ooi, K. *J. Mater. Chem.* **1999**, *9*, 319.
(4) Brock, S. L.; Sanabria, M.; Nair, J.; Suib, S. L.; Ressler, T. *J. Phys. Chem. B* **2001**, *105*, 5404.
(5) Armstrong, A. R.; Bruce, P. G. *Nature* **1996**, *381*, 499.
(6) Rao, C. N. R.; Cheetham, A. K.; Mahesh, R. *Chem. Mater.* **1996**, *8*, 2241.
(7) Tarascon, J. M.; Mckinnon, W. R.; Coowar, F.; Bowmer, T. N.; Amatucci, G.; Guyomard, D. *J. Electrochem. Soc.* **1994**, *141*, 1421.
(8) (a) Ching, S.; Petrovay, D. J.; Jorgensen, M. L.; Suib, S. L. *Inorg. Chem.* **1997**, *36*, 883. (b) Feng, Q.; Honbu, C.; Yanagisawa, K.; Yamasaki, N. *Chem. Mater.* **1999**, *11*, 2444. (c) Yang, X.-J.; Kanoh, H.; Tang, W.-P.; Liu, Z.-H.; Ooi, K. *Chem. Lett.* **2001**, 612. (d) Liu, Z.-H.; Ooi, K.; Kanoh, H.; Tang, W.-P.; Tomida, T. *Langmuir* **2000**, *16*, 4154.
(9) (a) Tian, Z.-R.; Tong, W.; Wang, J.-Y.; Duan, N.-G.; Krishnan, V. V.; Suib, S. L. *Science* **1997**, *276*, 926. (b) Ma, Y.; Suib, S. L.; Ressler, T.; Wong, J.; Lovallo, M.; Tsapatsis, M. *Chem. Mater.* **1999**, *11*, 3545. (c) Floros, N.; Michel, C.; Hervieu, M.; Raveau, B. *Chem. Mater.* **2000**, *12*, 3197.
(10) Wang, X.; Li, Y.-D. *J. Am. Chem. Soc.* **2002**, *124*, 2880.
(11) (a) Segal, S. R.; Park, S. H.; Suib, S. L. *Chem. Mater.* **1997**, *9*, 98. (b) Bayrachny, B.; Cheremskoy, P.; Gomozov, V.; Murovzev, L.; Skatkov, L. *Thin Solid Films* **1991**, *201*, L7.
(12) (a) Nishizawa, M.; Ise, T.; Koshika, H.; Itoh, T.; Uchida, I. *Chem. Mater.* **2000**, *12*, 1367. (b) Mallouk, T. E.; Gavin, J. A. *Acc. Chem. Res.* **1998**, *31*, 209.
(13) Long, J. W.; Qadir, L. R.; Stroud, R. M.; Rolison, D. R. *J. Phys. Chem. B* **2001**, *105*, 8712.
(14) Kanoh, H.; Tang, W.-P.; Makita, Y.; Ooi, K. *Langmuir* **1997**, *13*, 6845.
(15) Ratieuville, Y.; Wu, W.-L.; Lincot, D.; Vedel, J.; Yu, L.-T. *J. Electrochem. Soc.* **1999**, *146*, 3161.
(16) (a) Pang, S.-C.; Anderson, M. A.; Chapman, T. W. *J. Electrochem. Soc.* **2000**, *147*, 444. (b) Hu, C.-C.; Tsou, T.-W. *Electrochim. Acta.* **2002**, *47*, 3523.

10.1021/cm034191r CCC: $25.00
Published on Web 06/13/2003

with a thickness of submicrometers to micrometers. Various potential applications of these films for electroactive materials in rechargeable batteries, supercapacitors, and ion exchangers have been reported to date.[14−17]

The recently developed electrostatic self-assembly technique has provided an effective approach for the fabrication of a variety of ordered multilayer ultrathin films in layer-by-layer (LBL) fashion.[18] This strategy permits the assembly of different organic and inorganic building blocks into well-defined composite films with desired thickness and controlled architecture on a nanometer level. Recently, Suib et al. have prepared well-dispersed colloidal gels containing manganese oxide nanoparticles that were in the range of 2−8 nm in diameter.[19] By using these particles as inorganic building blocks, thin films of MnO_2 nanoparticles with a thickness of submicrometer range were successfully fabricated by the LBL self-assembly procedure.[20]

More recently, we have reported the synthesis, acid-exchange properties, swelling, and exfoliation behavior of a layered manganese oxide of A_xMnO_2, where A represents alkali metals such as Na and K.[21] Redoxable nanosheet crystallites of MnO_2 have been successfully obtained using tetrabutylammonium (TBA^+) ions as a delaminating agent. The resulting unilamellar crystallite consisting of a two-dimensional array of edge-shared MnO_6 octahedra has a crystallographic thickness of ca. 0.5 nm and a lateral dimension of submicrometers. It is of particular importance to develop a new kind of molecularly organized film with these novel manganese oxide nanosheets, because of the potential electrochemical or catalytic applications of their unique two-dimensional nature associated with a molecular thickness. Several groups have demonstrated the fabrication of multilayer ultrathin films incorporating insulating or semiconducting nanosheets.[22−24] However, there have been few reports on the fabrication of multilayer films of redoxable nanosheets. In this work, we report the fabrication and characterization of multilayer ultrathin films using the sequential LBL deposition of redoxable manganese oxide nanosheets and polycations.

Experimental Section

Reagents and Materials. Reagents such as K_2CO_3 (Wako Pure Chemical Co., Japan) and Mn_2O_3 (High Purity Chemical Co., Japan) of 99.9% purity were used as received in the synthesis of the starting layered manganese oxide of $K_{0.45}MnO_2$. A stoichiometric mixture of K_2CO_3 and Mn_2O_3 was heated at 800 °C for 30 h under an O_2 gas flow. X-ray diffraction (XRD) data of the obtained product of $K_{0.45}MnO_2$ agreed with that reported for $K_{0.47}Mn_{0.94}O_2$ in previous literature.[25] A protonic form of layered manganese oxide was prepared by digesting 10 g of $K_{0.45}MnO_2$ with 2 dm^3 of a 1 mol dm^{-3} HCl aqueous solution under stirring for 10 days. The HCl solution was refreshed every day to promote complete protonation. The resulting material was washed and air-dried at ambient temperature, yielding a protonic oxide with a composition of $H_{0.13}MnO_2 \cdot 0.7H_2O$.[21]

Polyethylenimine (PEI) (50% solution in water) and poly(diallyldimethylammonium) (PDDA) chloride (20% solution in water) were purchased from Aldrich and used without further purification. All other chemicals used were of analytical grade. Ultrapure water (resistivity >17 MΩ cm) from a Milli-Q water system was used throughout the experiments.

Exfoliation of Protonic $H_{0.13}MnO_2 \cdot 0.7H_2O$. A colloidal suspension of MnO_2 nanosheets was prepared by vigorously agitating 0.4 g of $H_{0.13}MnO_2 \cdot 0.7H_2O$ in 100 cm^3 of a tetrabutylammonium hydroxide ($(C_4H_9)_4NOH$) solution (5.2 mmol) at room temperature. After the suspension was shaken for 10 days, an unexfoliated component was separated by centrifugation at 10 000 rpm to obtain the colloidal suspension containing well-dispersed exfoliated nanosheets of manganese oxide.

Fabrication of Ultrathin Films. Substrates, such as Si wafers and quartz glass slides, were cleaned by treatment in a bath of methanol/HCl (1:1 in volume) and then concentrated H_2SO_4 for 15 min each. Indium-doped tin oxide (ITO)-coated glass slides were cleaned by ultrasonic washing in acetone. Ultrathin films were fabricated by applying the LBL assembly procedure similar to that described previously.[24] The substrates were precoated with PEI by immersion in an aqueous solution of PEI at pH 9 for 20 min. The PEI-primed substrates were then immersed in a colloidal suspension (0.02−0.16 g dm^{-3}, pH 8) of manganese oxide nanosheets for 20 min, followed by thorough washing with pure water, and then dipped in a solution of PDDA (pH 9, 20 g dm^{-3}) for 20 min and washed again. A series of these operations was repeated n times to obtain multilayer films of $PEI/MnO_2/(PDDA/MnO_2)_{n-1}$. The resulting films were dried with N_2 gas flow.

Characterizations. Ultraviolet−visible (UV−vis) spectra were recorded using a Hitachi U-4000 spectrophotometer equipped with an integrating sphere detection system. The surface topography of the films was visualized using a Seiko SPA400 atomic force microscopy (AFM) instrument in tapping mode with a silicon tip cantilever having a force constant of 20 N m^{-1}. XRD patterns were collected by a Rigaku Rint 2000 powder diffractometer with Cu Kα radiation ($\lambda = 0.15405$ nm). Fourier transform infrared (FT-IR) spectra were measured with a Digilab S-45 spectrometer in transmission mode by aligning a thin film on a silicon wafer substrate (5 × 6 cm^2) at a Brewster's angle of 75° with respect to the incident beam. X-ray photoelectron spectra (XPS) were recorded on a physical electronics XPS-5700 spectrometer with Al Kα X-ray line (1486.6 eV). The probing size was 0.8 mm in diameter. X-ray absorption near edge structure (XANES) spectra were obtained with synchrotron-radiated X-ray using an extended X-ray absorption fine-structure facility installed at beam line 12C at the photon factory in Tsukuba, Japan. The spectra for the films were obtained at room temperature in a total-reflection fluorescent mode using a 19 element Ge solid-state detector. The data for reference materials were taken in a transmission mode using gas-ionization detectors. Cyclic voltammograms were acquired in a three-electrode glass-cuvette cell with a Solartron SI-1287 computer-controlled potentiostat. A thin film of a PEI/MnO_2 layer pair deposited on the ITO glass slide was used as a working electrode, whereas an Ag/Ag^+ (0.01 M $AgNO_3$ in acetonitrile, 0.49 V vs standard hydrogen electrode) electrode and a glassy carbon were employed as reference and

(17) Giraldo, O.; Brock, S. L.; Willis, W. S.; Marquez, M.; Suib, S. L. *J. Am. Chem. Soc.* **2000**, *122*, 9330.
(18) (a) Decher, G. *Science* **1997**, *277*, 1232. (b) Fendler, J. H. *Chem. Mater.* **1996**, *8*, 1616. (c) Cassagneau, T.; Fendler, J. H.; Mallouk, T. E. *J. Am. Chem. Soc.* **1998**, *120*, 7848. (d) Caruso, F.; Möhwald, H. *J. Am. Chem. Soc.* **1999**, *121*, 6039.
(19) Brock, S. L.; Sanabria, M.; Suib, S. L.; Urban, V.; Thiyagarajan, P.; Potter, D. I. *J. Phys. Chem. B* **1999**, *103*, 7416.
(20) Lvov, Y.; Munge, B.; Giraldo, O.; Ichinose, I.; Suib, S. L.; Rusling, J. F. *Langmuir* **2000**, *16*, 8850.
(21) (a) Omomo, Y.; Sasaki, T.; Watanabe, M. *Solid State Ionics* **2002**, *151*, 243. (b) Omomo, Y.; Sasaki, T.; Wang, L. Z.; Watanabe, M. *J. Am. Chem. Soc.* **2003**, *125*, 3568.
(22) (a) Keller, S. W.; Kim, H.-N.; Mallouk, T. E. *J. Am. Chem. Soc.* **1994**, *116*, 8817. (b) Fang, M.-M.; Kaschak, D. M.; Sutorik, A. C.; Mallouk, T. E. *J. Am. Chem. Soc.* **1997**, *119*, 12184. (c) Schaak, R. E.; Mallouk, T. E. *Chem. Mater.* **2002**, *14*, 1455.
(23) (a) Cassagneau, T.; Guérin, F.; Fendler, J. H. *Langmuir*, **2000**, *16*, 7318. (b) Kotov, N. A.; Dékány, I.; Fendler, J. H. *Adv. Mater.* **1996**, *8*, 637. (c) Kotov, N. A.; Magonov, S.; Tropsha, E. *Chem. Mater.* **1998**, *10*, 886.
(24) (a) Sasaki, T.; Ebina, Y.; Watanabe, M.; Decher, G. *Chem. Commun.* **2000**, 2163. (b) Sasaki, T.; Ebina, Y.; Tanaka, T.; Harada, M.; Watanabe, M.; Decher, G. *Chem. Mater.* **2001**, *13*, 4661. (c) Sasaki, T.; Ebina, Y.; Fukuda, K.; Tanaka, T.; Harada, M.; Watanabe, M. *Chem. Mater.* **2002**, *14*, 3524.
(25) Delmas, C.; Fouassier, C. *Z. Anorg. Allg. Chem.* **1976**, *420*, 184.

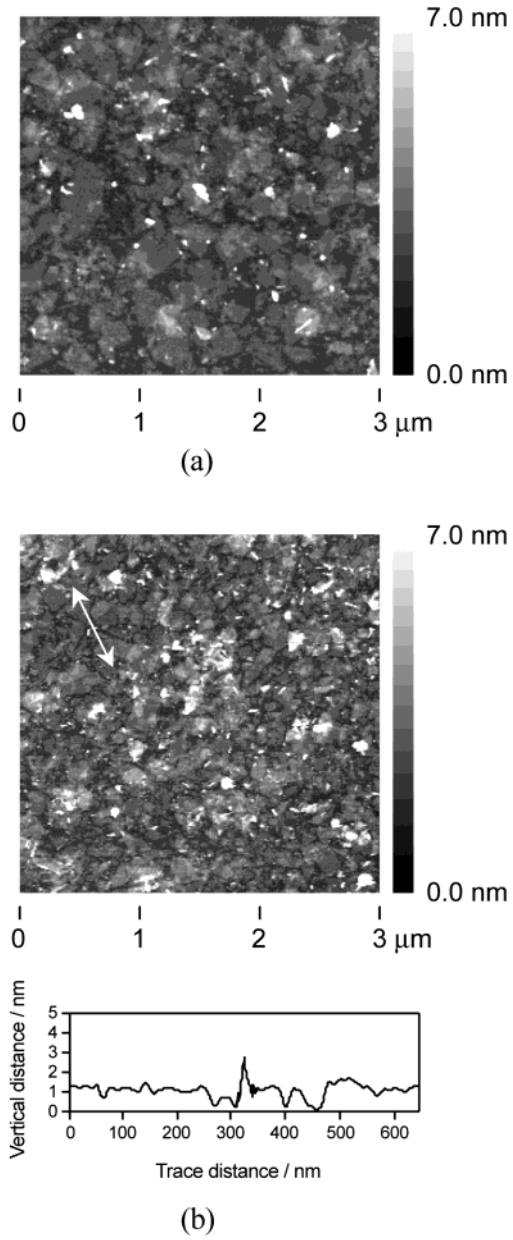

Figure 1. Tapping-mode AFM images of manganese oxide nanosheets deposited on PEI precoated Si wafer. Nanosheet concentration: (a) 0.04 g dm^{-3}, (b) 0.08 g dm^{-3}; pH value of solution = 9 for PEI and PDDA, and 8 for MnO_2 nanosheets; dipping time 20 min each. A cross-sectional analysis revealed the roughness in the film b indicated by an inserted arrow.

counter electrodes, respectively. Electrolyte (0.1 mol dm^{-3} $LiClO_4$ in propylene carbonate (PC)) was thoroughly degassed with N_2 gas bubbling prior to the experiments. CV experiments were performed from −1.3 to 0.9 V at a scan rate of 5−100 mV s^{-1}.

Results and Discussion

Self-Assembly of Multilayer Films. Figure 1 shows topographic images of the first deposited layer of manganese oxide nanosheets on a PEI-coated cationic surface of Si wafer. Although there were small uncovered areas and some overlapped patches, the surface was covered with irregularly shaped sheetlike crystallites, the dimensions of which ranged from 100 to several hundreds of nanometers. A section analysis revealed their nanosheet nature, showing an average thickness of 0.77 ± 0.05 nm.

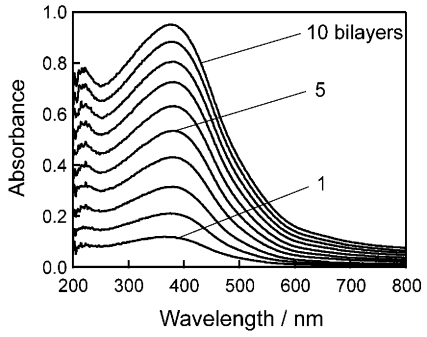

Figure 2. UV-vis absorption spectra of multilayer films of PEI/MnO_2/(PDDA/MnO_2)$_{n-1}$ prepared on quartz glass substrate. Nanosheet concentration: 0.08 g dm^{-3}; pH value of solution = 9 for PEI and PDDA, and 8 for MnO_2 nanosheets; deposition time was 20 min.

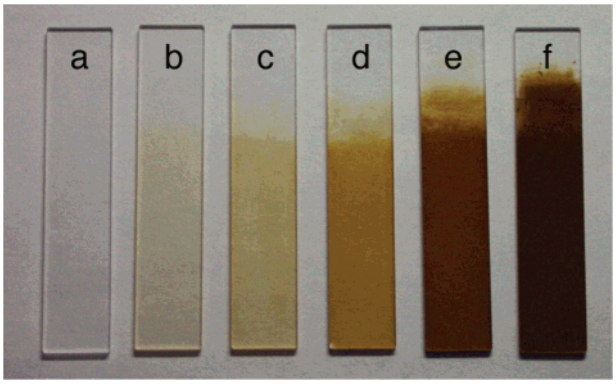

Figure 3. Photographs of thin films of PEI/MnO_2/(PDDA/MnO_2)$_{n-1}$ deposited on quartz glass substrates. Here, (a) represents bare substrate and (b) − (f) are films with n = 1, 2, 5, 10, 30, respectively.

The coverage tended to increase at higher suspension concentrations or with prolonged deposition time. A surface coverage of 87% was attained at the nanosheet concentration of 0.08 g dm^{-3} and the adsorption time of 20 min, while overlapping area of 39% was also formed. Quantitative analysis on the AFM image of this monolayer indicated that the standard vertical distance deviation was about 1.3 nm over the film area of 9 μm^2, suggesting the flat surface of the film. The overlapping of the nanosheets may be inevitable because of the large lateral size of the sheets. Some portion of the nanosheets may stick to bare cationic surface area whereas the bare area may not be large enough to arrange the sheet crystallite.

The subsequent growth of self-assembled thin films could be followed by UV−vis absorption spectra immediately after deposition of each bilayer (Figure 2). A photograph of the resulting films showing light-brown to deep-brown color is shown in Figure 3. A broad absorption band centered at around 380 nm is characteristic of manganese oxide nanosheets.[21b,27] Its absorbance increased almost linearly as a function of deposition numbers (Figure 4), indicating successful layer-

(26) Socrates, G. *Infrared Characteristic Group Frequencies*, 2nd ed.; John Wiley & Sons: Chichester, U.K., 1994.
(27) Ressler, T.; Brock, S. L.; Wong, J.; Suib, S. L. *J. Phys. Chem. B* **1999**, *103*, 6407.

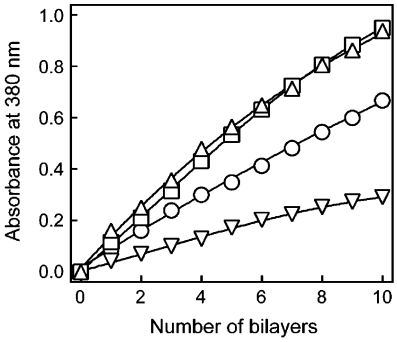

Figure 4. Dependence of absorbance at 380 nm in UV−vis spectra as a function of the deposition cycle. Nanosheet concentration: Δ, 0.16 g dm^{-3}; □, 0.08 g dm^{-3}; ○, 0.04 g dm^{-3}; ▽, 0.02 g dm^{-3}; pH value of solution = 9 for PEI and PDDA, and 8 for MnO_2 nanosheets; dipping time was 20 min each.

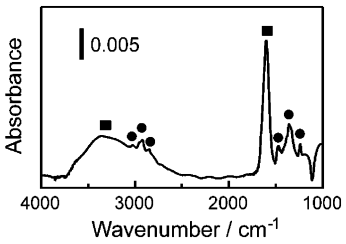

Figure 5. FT-IR spectra for as-prepared multilayer thin film of PEI/MnO_2/(PDDA/ MnO_2)$_9$. The squares and circles represent the signals arising from H_2O and PDDA, respectively.

by-layer growth. The enhancement was dependent upon the concentration of nanosheet suspension up to a value of 0.08 g dm^{-3}. In contrast, further increase in the nanosheet concentration had a negligible contribution to the absorbance, suggesting the saturation of adsorption was achieved. Similar behavior has been observed in other systems, such as a multilayer assembly of PDDA/$Ti_{0.91}O_2$ nanosheets.[24b] This may be because the nearly complete coverage of the substrate with negatively charged nanosheets prevents further adsorption due to the electrostatic repulsion. This charge neutralization/reversal upon adsorption of oppositely charged species is the underlying principle for the electrostatic self-assembly. The adsorption process is spontaneously terminated to attain a saturated loading, self-regulating the adsorption amount. Note that nearly full coverage was achieved at 0.08 g dm^{-3}, as shown in Figure 1b.

Characterizations. FT-IR spectra for multilayer films fabricated on Si wafer exhibited absorption bands that are characteristic of polycations used as a counterpart to the MnO_2 nanosheets in self-assembly (Figure 5); bands at around 3036, 2959, 2928, and 2866 cm^{-1} are assignable to the asymmetric and symmetric $-CH_2-$ and $-CH_3$ stretching bands for PDDA or PEI.[26] The bands at 1467 and 1356 cm^{-1} are attributable to the bending and deformation modes of the $-CH_2-$ group. The presence of hydrated water is indicated by a sharp bending vibration of water (ca. 1603 cm^{-1}) as well as its broad absorption (3700−3000 cm^{-1}) due to stretching.

The inorganic components in the film can be probed by XANES spectra. Figure 6 depicts the Mn K-edge profile for the thin film of PEI/MnO_2/(PDDA/MnO_2)$_9$ together with the data for its parent material of protonic $H_{0.13}MnO_2 \cdot 0.7H_2O$, and reference compounds of MnO_2 and Mn_2O_3. A pre-edge peak P was observed in each

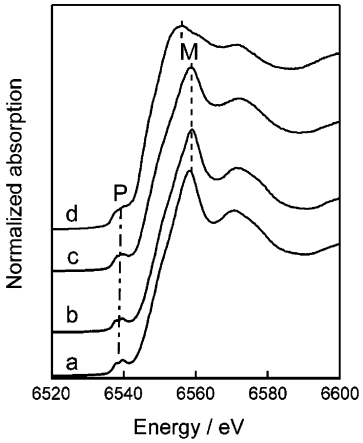

Figure 6. Mn K-edge XANES spectra for (a) as-prepared thin film of PEI/MnO_2/(PDDA/MnO_2)$_9$, (b) starting bulk material $H_{0.13}MnO_2 \cdot 0.7H_2O$, and references (c) MnO_2 and (d) Mn_2O_3. P and M represent the pre-edge peak and main peak in XANES, respectively.

spectra, which is assigned to the transition from the core 1s level to unoccupied 3d states.[27] Its weak intensity suggests that all manganese ions should be stabilized in an octahedral MnO_6 environment,[28] being compatible with the nanosheet structure. Strong absorption in the main-edge region of the spectra is associated with the dipole-allowed transitions from the core 1s level to unoccupied 4p states.[27] The multilayer thin film exhibited an edge energy of ∼6558 eV, which is approximately equal to that for the reference MnO_2 (6558 eV), but apparently different from that for Mn_2O_3. This suggests that the oxidation state of manganese in nanosheets is close to that in $Mn^{IV}O_2$. The chemical analysis indicated that the mean valence of manganese was 3.86−3.87 for the starting compound ($H_{0.13}MnO_2 \cdot 0.7H_2O$) before delamination and the restacked material of the exfoliated nanosheets.[21] This suggests that the oxidation state of manganese remains unchanged during exfoliation and the subsequent restacking process, which may also be true in the self-assembly process.

An XPS survey scan of the thin film of PEI/MnO_2/(PDDA/MnO_2)$_9$ detected N, O, Mn, and C in the films and/or substrate (Supporting Information I). The Mn (2p) region consisted of a spin−orbit doublet with an Mn ($2p_{1/2}$) binding energy of 653.7 eV and an Mn ($2p_{3/2}$) binding energy of 641.8 eV.[20] The C (1s) peak centered at 284.9 eV and N (1s) peak centered at 401.8 eV may be assignable to the carbon and nitrogen coming from polycation PDDA.[24c] The O (1s) peak was detected at a binding energy of 529.3 eV, which is characteristic of O bonded to Mn.[29] Quantification based on the XPS data indicated the atomic ratio N, 2.5%; O, 41.1%; Mn, 20.6%; and C, 32.1%. The Mn/O ratio of 1.99 is in excellent agreement with the stoichiometry of MnO_2. On the other hand, the C/N ratio deviated from its theoretical value

(28) (a) Hwang, S.-J.; Park, H.-S.; Choy, J.-H.; Campet, G. *J. Phys. Chem. B* **2001**, *105*, 335. (b) Hwang, S.-J.; Park, H.-S.; Choy, J.-H.; Campet, G. *Chem. Mater.* **2000**, *12*, 1818.

(29) (a) Moulder, J.; Stickle, W.; Sobol, P.; Bomben, K. *Handbook of X-ray Photoelectron Spectroscopy*; Chastain, J., Ed; Perkin-Elmer Corp.: Eden Prairie, MN, 1992. (b) *NIST X-ray Photoelectron Spectroscopy Database*; U. S. Secretary of Commerce; U.S. Government Printing Office: Washington, DC, 1997. (c) Wang, Z.-S.; Sasaki, T.; Muramastu, M.; Ebina, Y.; Tanaka, T.; Wang, L. Z.; Watanabe, M. *Chem. Mater.* **2003**, *15*, 807.

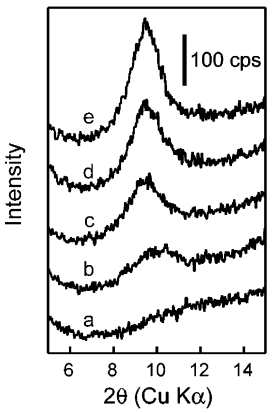

Figure 7. XRD pattern of as-prepared multilayer thin films of PEI/MnO_2/(PDDA/ MnO_2)$_{n-1}$. Here, n is 1 for (a), 3 for (b), 5 for (c), 10 for (d), and 15 for (e). The slant baseline is due to an amorphous halo from a quartz glass substrate appearing in a 2θ range of 10−35°.

of 8 for PDDA. A similar deviation has been frequently observed in XPS analysis,[24c,29] which can be ascribed to its high surface sensitivity to adsorbed carbonaceous species such as hydrocarbons. If we take a nitrogen signal for quantification of PDDA, the composition of the multilayer film is estimated to be $(PDDA)_{0.13}MnO_2$. Again, this is compatible with the mean valence of manganese estimated by XANES as well as chemical titration.

The XRD data for the obtained ultrathin films exhibited a Bragg peak centered at $2\theta = 9.6°$ and its peak intensity heightened successively with increasing deposition cycles (Figure 7). This diffraction feature can be accounted for by a nanostructure of repeating PDDA/MnO_2 bilayers. The average repeating distance was ca. 0.92 nm. Because the crystallographic thickness of MnO_2 nanosheets is 0.52 nm,[21b] the thickness of the PDDA layer is estimated to be 0.4 nm. A similar dimension has been reported for PDDA layer thickness in other systems.[24c] Recently, Liu et al. have reported the fabrication of a MnO_2/PDDA nanocomposite derived via flocculation of the delaminated MnO_2 sheets with PDDA.[30] The nanocomposite exhibited a large basal spacing of 1.54 nm, which has been accounted for by bilayers of PDDA in the MnO_2 gallery. Interestingly, different structures were resulted through two different routes, self-assembly and spontaneous restacking, with the same building blocks.

The Bragg peak in Figure 7 was fairly broad in comparison with a similar multilayer system of PDDA/$Ti_{0.91}O_2$ nanosheets,[24] which was characterized by its well-ordered multilayer structure. Smaller lateral size and possible buckling of the MnO_2 nanosheets may be responsible for the less crystalline nature.

All the characterization results support the formation of layer-by-layer assemblies of manganese oxide nanosheets and polycations. The obtained multilayer films may be one of the first molecularly organized systems based on manganese oxides in which their nanostructure and thickness can be tailored in a subnanometer to nanometer regime. Most of the films of manganese oxides fabricated by sol−gel methods have a thickness

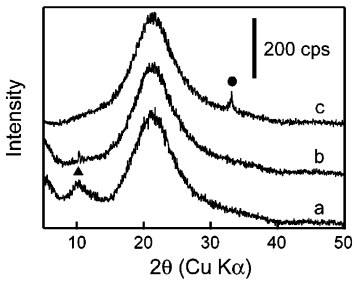

Figure 8. XRD patterns of the thin film of PEI/MnO_2/(PDDA/MnO_2)$_9$ heated at different temperatures: a, 100 °C × 1 h; b, 200 °C × 1 h; c, 600 °C × 1 h. The square and circle represent a basal reflection of PDDA/MnO_2 multilayer and the 222 peak of Mn_2O_3, respectively.

of submicrometers to micrometers. Self-assembly of manganese oxide nanoparticles reported by Lvov et al. allowed film thickness control in a range of 20−40 nm.[20] In contrast, the multilayer assemblies in the present study have much finer controllability over their film architecture.

Heat Treatments. The structural evolution of the multilayer film of PEI/MnO_2/(PDDA/MnO_2)$_9$ upon heating at different temperatures is shown in Figure 8. A broad hump centered at around 21.5° (2θ) in each XRD pattern is attributable to the quartz glass substrate. The diffraction peak of $d \approx 0.9$ nm remained almost unchanged at 100 °C, indicating the intactness of the inorganic−organic multilayer structure. Heating at higher temperatures resulted in the loss of this peak. The collapse of an ordered inorganic/organic bilayer structure may be induced by the elimination of organic species. Upon heating at 500 °C, a new XRD peak appeared at around 33° (2θ) and this peak tended to enhance with increasing temperature. Although the faint signal from the ultrathin film makes it difficult to realize conclusive identification, this diffraction peak may be attributable to the 222 reflection of Mn_2O_3.[31] Thermal degradation of a layered protonic oxide of $H_{0.13}MnO_2 \cdot 0.7H_2O$ produced polycrystalline Mn_2O_3 having a diffraction line at 33° in 2θ as the strongest. Actually, the XANES data (Supporting Information II) were very similar to those for Mn_2O_3.

Electrochemical Properties. The cyclic voltammogram of a monolayer ITO/PEI/MnO_2 electrode (Figure 9) exhibited a pronounced reduction peak at −0.66 V vs Ag/Ag^+ on the negative going sweep, whereas two oxidation peaks at −0.36 and 0.23 V vs Ag/Ag^+ were exhibited on the positive going sweep. This indicates that the nanosheet film undergoes a reduction reaction in one step and an oxidation process in two steps. Note that the bare ITO itself and PEI-primed ITO did not show any redox peak in this scan range. The peak current increased linearly with increasing scan rate from 5 mV s^{-1} to 100 mV s^{-1}, suggesting that the electroactive species of MnO_2 nanosheets adsorbed on the electrode are responsible for the redox processes. The electron transfers were estimated to be $\sim 1.8 \times 10^{-9}$ mol cm^{-2} (170−180 μC cm^{-2}) for both the reduction and the oxidation reactions from the integrated peak areas of the second cycle. The MnO_2 nanosheets have a hexagonal two-dimensional unit cell ($a \sim 0.3$ nm) that

(30) Liu, Z.-H.; Yang, X.-J.; Makita, Y.; Ooi, K. *Chem. Mater.* **2002**, *14*, 4800.

(31) JCPDS 41-1442.

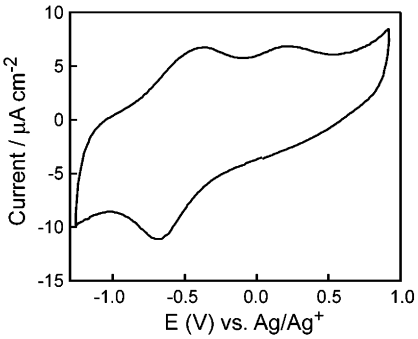

Figure 9. Cyclic voltammogram of a monolayer film of PEI/MnO_2 on ITO glass slide in 0.1 mol dm^{-3} $LiClO_4$/PC electrolyte (scan rate 10 mV s^{-1}; potential range −1.3 V − 0.9 V; second cycle). The scan started from the rest potential ($E_{Ag/Ag^+} = -0.1$ − 0.1 V) to a negative direction.

contains one formula weight of MnO_2. If we assume that the electrode surface was covered with a perfect monolayer, a deposited amount of the nanosheets is estimated to be $\sim 2.1 \times 10^{-9}$ mol cm^{-2}.[32] This is close to 1:1 in molar ratio compared with that for electron transfers during CV, indicating that a dominant amount of the manganese oxide on the electrode may be electroactive. These redox peaks should be attributable to the electrochemical conversion between Mn^{IV} and Mn^{III} in the film.

The CV characteristics of manganese oxide in terms of redox potentials and currents are highly dependent on the crystal structures and composition of the materials,[1,14,33,34] which can be employed for characterizing and distinguishing manganese oxides with various forms.[1,34] The data demonstrated in this study provide a new example for CV measurements and can be taken as characteristics for the fundamental units of the layered systems, which may be important to arrive at a deeper understanding of electrochemical behaviors of "nanosized" crystallites as well as bulk layered hosts. Further study on the electrochemical properties of the thin films is now in progress and will be published elsewhere.

In summary, multilayer ultrathin films composed of novel manganese oxide nanosheets and polycations have been successfully fabricated on various substrates using the sequential LBL procedure. Various characterizations support the layer-by-layer formation of organic−inorganic nanocomposite films, which could finally be converted to inorganic manganese oxide films upon heat treatment. Cyclic voltammogram data demonstrated the electrochemical redox behavior of the MnO_2 nanosheets.

Acknowledgment. The XANES experiments were performed under the approval of the photon factory program advisory committee (2001G324).

Supporting Information Available: Survey XPS data for an as-prepared multilayer thin film of PEI/MnO_2/(PDDA)/$MnO_2)_9$ and Mn K-edge XANES spectra for multilayer thin films of PEI/MnO_2/(PDDA/$MnO_2)_9$ heated at different temperatures (PDF). These materials are available free of charge via the Internet at http://pubs.acs.org.

CM034191R

(32) The unit cell area S_{uc} is 0.078 nm^2 (= 0.3 × 0.3 × sin120°). The deposited amount M can be calculated as: $M = 1/(N_a \times S_{uc})$, where N_a is Avogadro's number.

(33) Chromik, R.; Beck, F. *Electrochim. Acta*, **2000**, *45*, 2175.

(34) De Guzman, R. N.; Shen, Y.-F.; Shaw, B. R.; Suib, S. L.; O'Young, C. L. *Chem. Mater.* **1993**, *5*, 1395.